

**AFRL-ML-WP-TP-2006-504**

**DEVELOPMENT OF LOW DENSITY  
CaMg-Al-BASED BULK METALLIC  
GLASSES (Preprint)**



**O.N. Senkov, J.M. Scott, and D.B. Miracle**

**OCTOBER 2006**

**Approved for public release; distribution is unlimited.**

**STINFO COPY**

**This work, resulting in whole or in part from department of the Air Force contract number FA8650-04-D-5233, has been submitted to Elsevier for publication in the Journal of Alloys and Compounds. If this work is published, Elsevier may assert copyright. The United States has for itself and others acting on its behalf an unlimited, paid-up, nonexclusive, irrevocable worldwide license to use, modify, reproduce, release, perform, display, or disclose the work by or on behalf of the government. All other rights are reserved by the copyright owner.**

**MATERIALS AND MANUFACTURING DIRECTORATE  
AIR FORCE RESEARCH LABORATORY  
AIR FORCE MATERIEL COMMAND  
WRIGHT-PATTERSON AIR FORCE BASE, OH 45433-7750**

REPORT DOCUMENTATION PAGE				Form Approved OMB No. 0704-0188	
The public reporting burden for this collection of information is estimated to average 1 hour per response, including the time for reviewing instructions, searching existing data sources, gathering and maintaining the data needed, and completing and reviewing the collection of information. Send comments regarding this burden estimate or any other aspect of this collection of information, including suggestions for reducing this burden, to Department of Defense, Washington Headquarters Services, Directorate for Information Operations and Reports (0704-0188), 1215 Jefferson Davis Highway, Suite 1204, Arlington, VA 22202-4302. Respondents should be aware that notwithstanding any other provision of law, no person shall be subject to any penalty for failing to comply with a collection of information if it does not display a currently valid OMB control number. PLEASE DO NOT RETURN YOUR FORM TO THE ABOVE ADDRESS.					
1. REPORT DATE (DD-MM-YY) October 2006		2. REPORT TYPE Journal Article Preprint		3. DATES COVERED (From - To)	
4. TITLE AND SUBTITLE DEVELOPMENT OF LOW DENSITY CaMg-A1-BASED BULK METALLIC GLASSES (Preprint)				5a. CONTRACT NUMBER FA8650-04-D-5233	
				5b. GRANT NUMBER	
				5c. PROGRAM ELEMENT NUMBER 62102F	
6. AUTHOR(S) O.N. Senkov and J.M. Scott, (UES, Inc.) D.B. Miracle (Metals Branch (AFRL/MLLM))				5d. PROJECT NUMBER 2311	
				5e. TASK NUMBER 00	
				5f. WORK UNIT NUMBER 23110002	
7. PERFORMING ORGANIZATION NAME(S) AND ADDRESS(ES)  UES, Inc 4401 Dayton-Xenia Road Dayton, OH 45432				8. PERFORMING ORGANIZATION REPORT NUMBER	
Metals Branch (AFRL/MLLM) Metals, Ceramics and Nondestructive Evaluation Division Materials and Manufacturing Directorate Air Force Research Laboratory, Air Force Materiel Command Wright-Patterson AFB, OH 45433-7750					
9. SPONSORING/MONITORING AGENCY NAME(S) AND ADDRESS(ES)  Materials and Manufacturing Directorate Air Force Research Laboratory Air Force Materiel Command Wright-Patterson AFB, OH 45433-7750				10. SPONSORING/MONITORING AGENCY ACRONYM(S) AFRL-ML-WP	
				11. SPONSORING/MONITORING AGENCY REPORT NUMBER(S) AFRL-ML-WP-TP-2006-504	
12. DISTRIBUTION/AVAILABILITY STATEMENT Approved for public release; distribution is unlimited.					
13. SUPPLEMENTARY NOTES Submitted for publication in the Journal of Alloys and Compounds, publisher: Elsevier. PAO Case Number: AFRL/WS 06-2304, 27 September 2006.					
14. ABSTRACT Low density Ca-Mg-Al-based bulk metallic glasses containing additionally Cu and Zn, were produced by a copper mold casting method as wedge-shaped samples with thicknesses varying from 0.5 mm to 10 mm. The compositions of the alloys were selected using recently developed specific criteria for glass formation. A structural assessment using the efficient cluster packing model was also applied and showed a good ability to represent these glasses. Thermal properties of the new metallic glasses, such as the glass transition, crystallization and melting temperatures, as well as heats of crystallization and melting are reported. The critical cooling rate for amorphization and the fragility index are estimated for these alloys. The effect of the alloy composition on glass forming ability is discussed.					
15. SUBJECT TERMS					
16. SECURITY CLASSIFICATION OF:			17. LIMITATION OF ABSTRACT: SAR	18. NUMBER OF PAGES 22	19a. NAME OF RESPONSIBLE PERSON (Monitor) Daniel B. Miracle 19b. TELEPHONE NUMBER (Include Area Code) (937) 255-1305
a. REPORT Unclassified	b. ABSTRACT Unclassified	c. THIS PAGE Unclassified			

# Development of Low Density Ca-Mg-Al- Based Bulk Metallic Glasses

O.N. Senkov\*<sup>#</sup>, J.M. Scott\* and D.B. Miracle

Air Force Research Laboratory, Materials and Manufacturing Directorate, Wright-Patterson AFB, OH 45433, USA; \*UES, Inc., 4401 Dayton-Xenia Rd., Dayton, OH 45433, USA

## Abstract

Low density Ca-Mg-Al-based bulk metallic glasses containing additionally Cu and Zn, were produced by a copper mold casting method as wedge-shaped samples with thicknesses varying from 0.5 mm to 10 mm. The compositions of the alloys were selected using recently developed specific criteria for glass formation. A structural assessment using the efficient cluster packing model was also applied and showed a good ability to represent these glasses. Thermal properties of the new metallic glasses, such as the glass transition, crystallization and melting temperatures, as well as heats of crystallization and melting are reported. The critical cooling rate for amorphization and the fragility index are estimated for these alloys. The effect of the alloy composition on glass forming ability is discussed.

## Introduction

Ca-Mg-based bulk metallic glasses are relatively new class of amorphous alloys, which attract interest of several research groups for their unique properties [1-10]. In particular, these metallic glasses have the lowest density ( $\sim 2.0$  g/cc) among all known amorphous metallic alloys. They also have low Young's modulus ( $\sim 20-35$  GPa) [11] comparable to the modulus of human bones, low glass transition temperature ( $T_g \sim 100-150^\circ\text{C}$ ) and a wide temperature range of super-cooled liquid ( $\Delta T_{xg} = T_x - T_g \sim 30-70$  °C). It is also noteworthy that these glassy alloys are based on two simple metals, Ca and Mg, which distinguishes them from all other transition-metal based bulk

---

<sup>#</sup> Corresponding author. Address: UES, Inc., 4401 Dayton-Xenia Rd., Dayton, OH 45432-1894, USA; E-mail: oleg.senkov@wpafb.af.mil.

metallic glasses [12], and most of these Ca-Mg-based glasses were produced using specific topological and thermodynamic criteria for glass formation, which have recently been developed at the Air Force Research Laboratory [5,13-19]. By applying these new criteria to Ca-based alloy systems, favorable glass formation was predicted in the alloys described by formula:



where  $A=0.40-0.70$ ;  $B=0-0.25$ ;  $C=0-0.25$ ;  $D=0-0.35$ ;  $E=0-0.35$ ;  $B+C+D \geq 0.05$ ;  $A+B+C+D+E=1$ ; and  $Ln$  represents a metal from the lanthanide group. A strong topological basis exists for the compositions represented in Equation (1) [13-18], which are also well described by a recently developed structural model for metallic glasses [19].

The main drawback of the Ca-based metallic alloys is their poor oxidation and corrosion resistance. Many Ca-based crystalline alloys are very reactive, even in pure water, and oxidize in air in a matter of days. Transition in the amorphous state considerably improves the oxidation and corrosion resistance of these alloys, although these properties also depend on the alloy constitution [20-22]. For example, recent studies of four Ca-Mg-Zn, Ca-Mg-Cu, Ca-Mg-Zn-Cu and Ca-Mg-Al-Zn-Cu metallic glasses have shown that the ternary Ca-Mg-Zn glass has the least oxidation and corrosion resistance. Substitution of Zn with Cu and/or Al improves these properties, and the alloy containing Al has the best oxidation and corrosion resistance [22]. Several Ca-Al-based bulk metallic glasses have recently been reported [7]; however, these glasses have not very good glass forming ability and the maximum diameter of fully amorphous rods made of these alloys by a water cooled copper mold casting method generally does not exceed 2 mm. Only two of the reported amorphous alloys,  $\text{Ca}_{56.5}\text{Mg}_{10}\text{Al}_{28.5}\text{Cu}_5$  and  $\text{Ca}_{56.5}\text{Mg}_{10}\text{Al}_{28.5}\text{Cu}_5$ , had a higher maximum diameter of 3 mm [7].

In the present work we report on several new Ca-Mg-Al-based amorphous alloys with better glass forming ability. The compositions of these alloys were selected using Equation (1) and recently developed specific criteria for glass formation. Thermal properties of the new metallic glasses, such as the glass transition, crystallization and melting temperatures, as well as heats of crystallization and melting are reported. The effect of the alloy constitution on glass forming ability and glass stability is discussed.

### **Experimental**

Several Ca-Mg-Al-based alloys, which nominal composition is shown in Table 1, were prepared by induction melting of mixtures of pure elements (99.99% for Al and Cu, 99.9% for Mg and Zn,



and 99.5% for Ca) in a water-cooled copper crucible in an argon atmosphere. Each of the produced alloys was then induction re-melted in a quartz crucible with a 12.5 mm inner diameter and an ~2 mm diameter hole in the bottom of the crucible and cast through this hole into a water-cooled copper mold to produce wedge-like samples of two different dimensions. One type of samples had 6.4 mm width, 35 mm height, and thickness varying from 0.5 mm at the base of the wedge to 3.5 mm at the top of the wedge. Another type of samples had 11 mm width, 50 mm height, and thickness varying from 2 mm at the base of the wedge to 10 mm at the top of the wedge. The time to fill the mold cavity was about 0.5 seconds for smaller samples and ~1.0-1.5 seconds for larger samples. The amorphous or crystalline structure of the cast alloys was identified by X-ray diffraction of powdered samples using a Rigaku Rotaflex diffractometer, Cu  $K_{\alpha}$  radiation, and a differential scanning calorimeter (DSC) Q1000, By TA Instruments, Inc. The glass transition,  $T_g$ , and crystallization,  $T_x$ , temperatures, the temperatures of start,  $T_m$ , and completion,  $T_f$ , of melting, and heats of crystallization,  $\Delta H_x$ , of the cast alloys were determined using DSC scans at a heating rate of 40 K/min. The maximum thickness,  $\tau_{max}$ , at which an alloy remained fully amorphous after the water-cooled copper mold casting, was determined using X-ray diffraction and DSC patterns of several samples extracted from different-thickness regions of the wedge specimens as a thickness above which  $\Delta H_x$  starts to decrease from its maximum value and sharp peaks from crystalline phases appear on the X-ray diffraction patterns. This method is described elsewhere [8]. The weight of samples used for DCS was in the range of 6 to 15 mg.

## Results

**Ternary Alloys.** The ternary alloys were produced with the concentrations of Ca varying from 50 to 75 at.% and the concentration of Al varying from 4 to 35 at.% (Table 1). The density of these alloys increases from 1.62 g/cc to 1.79 g/cc with a decrease in the concentration of Ca and an increase in the concentration of Al. Seven of nine produced ternary Ca-Mg-Al alloys have marginal glass forming ability, and the maximum amorphous thickness,  $\tau_{max}$ , of these alloys after casting in a wedge cavity does not exceed 0.5 mm (see Table 1). Two other ternary alloys,  $Ca_{65}Mg_{15}Al_{20}$  and  $Ca_{70}Mg_{15}Al_{15}$ , have better glass forming ability and show  $\tau_{max}$  of 1.0 mm and 1.5 mm, respectively. Typical X-ray diffraction patterns and DSC heating curves for the ternary alloys in fully amorphous and partially amorphous conditions are shown in Figures 1(a) and 2(a-b), respectively. Three alloy groups with different crystallization kinetics can be recognized. The

first group consists of one glassy alloy,  $\text{Ca}_{55}\text{Mg}_{15}\text{Al}_{30}$ . A DSC pattern of this alloy shows two exothermic crystallization reactions near  $283^\circ\text{C}$  and  $386^\circ\text{C}$  and at least two endothermic reactions due to alloy melting, with the reaction peaks at  $495^\circ\text{C}$  and  $540^\circ\text{C}$  (see Figure 2). A shallow endothermic reaction is also recognized in the temperature range between  $225^\circ\text{C}$  and  $282^\circ\text{C}$  ( $\Delta T_x = 57^\circ\text{C}$ ), which is due to transition of the glass into a super-cooled liquid state.

The second group consists of three alloys,  $\text{Ca}_{62}\text{Mg}_9\text{Al}_{29}$ ,  $\text{Ca}_{60}\text{Mg}_{15}\text{Al}_{25}$ , and  $\text{Ca}_{65}\text{Mg}_{15}\text{Al}_{20}$ . For these alloys, only one sharp crystallization peak is observed, which shifts to a lower temperature range and becomes sharper and more intense with a decrease in the amount of Al. The super-cooled liquid range for this alloys is rather narrow ( $\Delta T_x = 36^\circ\text{C}$ ,  $26^\circ\text{C}$ , and  $20^\circ\text{C}$ , respectively), and the melting temperature gradually decreases to an eutectic point at  $\sim 410\text{-}415^\circ\text{C}$  (see Figure 2 and Table 1). During melting these alloys experience at least two phase transformations, which result in two sharp endothermic peaks.

In the third group, which consists of  $\text{Ca}_{70}\text{Mg}_{15}\text{Al}_{15}$ ,  $\text{Ca}_{70}\text{Mg}_{26}\text{Al}_4$ ,  $\text{Ca}_{72.5}\text{Mg}_{12.5}\text{Al}_{15}$ , and  $\text{Ca}_{75}\text{Mg}_{15}\text{Al}_{10}$ , several wide overlapped crystallization peaks are observed in the temperature range of  $180^\circ\text{C}$  to  $280^\circ\text{C}$  (see Figures 2a and 2b). Melting of these alloys starts at the same temperature of about  $360^\circ\text{C}$  and the enthalpy of the first melting peak is very low, about  $8.3\text{ J/g}$ . The second melting peak is much more intense,  $\Delta H_m \approx 125\text{ J/g}$ , and it starts also at near the same temperature of  $\sim 414^\circ\text{C}$  for these alloys. It is likely that the weak peak at  $360^\circ\text{C}$  is due to melting of a metastable eutectic and the sharp peak at  $\sim 414^\circ\text{C}$  is due to melting of an equilibrium eutectic, which follows by a gradual melting of a primary phase with an increase in the temperature up to  $480\text{-}510^\circ\text{C}$ .

At a constant Mg content, the glass transition, crystallization and melting temperatures for the ternary Ca-Mg-Al alloys have a tendency to decrease with a decrease in the amount of Al and an increase in the amount of Ca in the concentration range of Ca from 50% to 75% (see Table 1). For example,  $T_g$  decreases from  $\sim 240^\circ\text{C}$  to  $130^\circ\text{C}$  and  $T_x$  decreases from  $\sim 280^\circ\text{C}$  to  $150^\circ\text{C}$  in this composition range. There is, however, no correlation between the maximum amorphous thickness,  $\tau_{\text{max}}$ , and the temperature range of the super-cooled liquid,  $\Delta T_x = T_x - T_g$ , which is used as a measure of glass stability, or other empirical glass forming ability parameters such as  $T_g/T_l$  or  $T_x/(T_g + T_l)$ . However, it can be noted from Table 1 that there is a tendency for  $\tau_{\text{max}}$  to increase with a decrease in the melting range  $\Delta T_m = T_l - T_m$ .



**Quaternary alloys.** Two type quaternary alloys were produced, i.e. Ca-Mg-Al-Zn and Ca-Mg-Al-Cu (see Table 1). Typical X-ray diffraction patterns of one of these alloys,  $\text{Ca}_{60}\text{Mg}_{15}\text{Al}_{10}\text{Zn}_{15}$ , versus the alloy thickness are shown in Figure 1b. These patterns illustrate transition of the alloy from a fully amorphous to a partially crystalline state with an increase in the alloy thickness from 4 mm to 10 mm. The Zn containing glassy alloys contain 48 to 60 at.% Ca, 13 to 20 at.% Mg, 10 to 20 at.% Al, and 6 to 20 at.% Zn and their typical DSC curves are shown in Figure 3. The Cu-containing alloys have 50 or 60 at.% Ca, 9 to 22.5 at.% Mg, 5 to 11 at. % Al, and 10 to 22.5 at.% Cu and their DSC curves are given in Figure 4. The density of these alloys varies from 1.84 to 2.27 g/cc. The density increases with an increase in the amounts of Cu or Zn, and, in a smaller extent, Al and Mg. Ternary Ca-Mg-Zn and Ca-Mg-Cu bulk amorphous alloys recently reported elsewhere [8,23], which have a very good glass forming ability ( $\tau_{\text{max}} = 10$  mm), were used as a baseline to design these quaternary metallic glasses by partial substitution of the alloying elements (mainly Zn or Cu) with Al. The Al addition to these ternary alloys reduces the maximum amorphous thickness; however, it increases glass stability by increasing both  $T_g$  and  $T_x$ . (For the Ca-Mg-Zn and Ca-Mg-Cu alloys,  $T_g$  and  $T_x$  values change from 80 to 130°C and from 112°C to 170°C, respectively, depending on the alloy composition [8,23].)

The Cu containing alloys have the critical amorphous thickness within 1 to 3.5 mm range, while the Zn containing alloys have  $\tau_{\text{max}}$  from 1 to 5 mm. When the specimen thickness  $\tau$  exceeds  $\tau_{\text{max}}$ , the volume fraction of the amorphous phase generally rapidly decreases to zero with a further increase in  $\tau$  [8,23]. However, in two alloys,  $\text{Ca}_{60}\text{Mg}_{15}\text{Al}_{10}\text{Zn}_{15}$  and  $\text{Ca}_{60}\text{Mg}_{20}\text{Al}_{10}\text{Zn}_{10}$ , the volume fraction of the amorphous phase, as estimated from the intensities of the X-ray diffraction peaks and the DSC exothermic peaks, remains above 80% in the specimens with thicknesses of up to 10 mm and 8 mm, respectively. In Ca-Mg-Al-Zn alloys,  $T_g$  varies from 130°C to 175°C,  $T_x$  varies from 176°C to 218°C and both  $T_g$  and  $T_x$  have a tendency to increase with an increase in the Al content. The Ca-Mg-Al-Cu alloys have smaller values of  $T_g$  (124°C to 143°C) and  $T_x$  (157°C to 183°C) and, therefore, lower glass stability than the Ca-Mg-Al-Zn alloys. The temperature range of a super-cooled liquid for these quaternary alloys is rather large. For example, in Zn-containing alloys it varies from  $\Delta T_x = 36^\circ\text{C}$  in  $\text{Ca}_{55}\text{Mg}_{20}\text{Al}_{19}\text{Zn}_6$  to  $71^\circ\text{C}$  in  $\text{Ca}_{60}\text{Mg}_{15}\text{Al}_{10}\text{Zn}_{15}$ . In Cu-containing alloys,  $\Delta T_x$  is between  $30^\circ\text{C}$  and  $49^\circ\text{C}$ .

Crystallization of these quaternary amorphous alloys is accompanied by a single or multiple exothermic reactions, depending on the alloy composition (see Figures 3 and 4). Melting of these

alloys occurs in a rather wide temperature range and is generally accompanied with several endothermic peaks. For example, the  $\text{Ca}_{60}\text{Mg}_{20}\text{Al}_{10}\text{Zn}_{10}$  glass, which has the best glass forming ability ( $\tau_{\text{max}} = 5$  mm), has  $\Delta T_1 = T_1 - T_m = 139^\circ\text{C}$ , and the second best glass former,  $\text{Ca}_{60}\text{Mg}_{15}\text{Al}_{10}\text{Zn}_{15}$ , has  $\Delta T_1 = 80^\circ\text{C}$ . It is well established for many glass forming systems, including Ca-Mg-Zn [8,24] and Ca-Mg-Cu [23], that the best glass forming alloys have a near-eutectic composition and slow crystallization kinetics. The fact that the majority of the developed Ca-Mg-Al-Zn and Ca-Mg-Al-Cu glassy alloys have a very wide melting range indicate that their compositions are far from the eutectic composition, and even better glass forming ability and larger maximum amorphous thicknesses are expected in optimized alloy compositions with a considerably reduced melting range.

**Quintenary Ca-Mg-Al-Zn-Cu alloys.** The composition of five quintenary metallic glasses produced in this work is given in Table 1 and their DSC patterns are shown in Figure 5. A very good glass forming alloy,  $\text{Ca}_{55}\text{Mg}_{18}\text{Zn}_{11}\text{Cu}_{16}$ , which has been reported to have a maximum amorphous thickness  $\tau_{\text{max}} > 10$  mm [10], was used as a starting point, and from 5 to 15 % Al, as well as up to 5% Ca, were added to this alloy to partially substitute Cu and Zn and reduce the density. Without Al, this alloy has  $T_g$  and  $T_x$  of  $100^\circ\text{C}$  and  $166^\circ\text{C}$ , respectively, and the density of 2.32 g/cc. Substitution of every 1 at.% of Cu and/or Zn with Al and Ca decreases the density of this alloy by  $\sim 1\%$  and  $1.5\%$ , respectively. For example, the densities of  $\text{Ca}_{55}\text{Mg}_{18}\text{Al}_{15}\text{Zn}_6\text{Cu}_6$  and  $\text{Ca}_{60}\text{Mg}_{18}\text{Al}_{15}\text{Zn}_3\text{Cu}_4$  alloys are 1.99 g/cc and 1.84 g/cc, respectively (see Table 1). However, glass forming ability rapidly reduces with Al addition. For example, partial replacement of Cu in  $\text{Ca}_{55}\text{Mg}_{18}\text{Zn}_{11}\text{Cu}_{16}$  with 5 at.% Al decreases the  $\tau_{\text{max}}$  to 9 mm in a  $\text{Ca}_{55}\text{Mg}_{18}\text{Al}_5\text{Zn}_{11}\text{Cu}_{11}$  alloy. A further increase in Al to 10 and 15 at.% decreases  $\tau_{\text{max}}$  to 3 mm and 2.5 mm, respectively, in  $\text{Ca}_{55}\text{Mg}_{18}\text{Al}_{10}\text{Zn}_{11}\text{Cu}_6$  and  $\text{Ca}_{55}\text{Mg}_{18}\text{Al}_{15}\text{Zn}_6\text{Cu}_6$  alloys. At the same time, substitution of 5 at.% Al with Ca in the latter alloy leads to a  $\text{Ca}_{60}\text{Mg}_{18}\text{Al}_{10}\text{Zn}_6\text{Cu}_6$  alloy with doubled glass forming ability ( $\tau_{\text{max}} = 5$  mm) and lower density of 1.94 g/cc (see Table 1). X-ray diffraction patterns of this alloy at different thicknesses are shown in Figure 1c. Only a diffuse amorphous halo is present at  $t$  up to 5mm; however, a number of peaks from crystalline phases are present on the X-ray diffraction pattern from a 7-mm thick region. Although it reduces the glass forming ability, addition of Al considerably improves the glass stability by increasing  $T_g$  and  $T_x$  (see Table 1 and Figure 5). For example, in the alloy  $\text{Ca}_{55}\text{Mg}_{18}\text{Al}_{15}\text{Zn}_6\text{Cu}_6$   $T_g$  and  $T_x$  are about  $36^\circ\text{C}$  and  $11^\circ\text{C}$



higher than in  $\text{Ca}_{55}\text{Mg}_{18}\text{Zn}_{11}\text{Cu}_{16}$ . The temperature range of super-cooled liquid has a tendency to slightly decrease with an increase in Al and it is in the range of  $\Delta T_x = 41 - 56^\circ\text{C}$ .

Addition of Al changes the crystallization and melting patterns of the  $\text{Ca}_{55}\text{Mg}_{18}\text{Zn}_{11}\text{Cu}_{16}$  glassy alloy (see Figure 6). Crystallization of the amorphous alloy without Al starts at  $\sim 166^\circ\text{C}$  and produces a sharp exothermic peak with a maximum at  $\sim 171^\circ\text{C}$ , which is followed by a smaller exothermic peak at  $\sim 210^\circ\text{C}$ . Melting of this alloy occurs in a rather narrow temperature range by a single endothermic reaction, indicating that the alloy may have a near eutectic composition. When 5% Cu is substituted by Al ( $\text{Ca}_{55}\text{Mg}_{18}\text{Al}_5\text{Zn}_{11}\text{Cu}_{11}$  alloy), both crystallization peaks become wider and their maxima occur at higher temperatures,  $184^\circ\text{C}$  and  $235^\circ\text{C}$ , respectively. Such behavior indicates that Al slows down the crystallization kinetics. Melting also occurs at higher temperatures and is accompanied by multiple endothermic reactions within about twice wider temperature range in the melting range.

The first crystallization reaction suppresses to a larger extent with further addition of Al up to 10 and 15 at.% in place of Cu and Zn ( $\text{Ca}_{55}\text{Mg}_{18}\text{Al}_{10}\text{Zn}_{11}\text{Cu}_6$  and  $\text{Ca}_{55}\text{Mg}_{18}\text{Al}_{15}\text{Zn}_6\text{Cu}_6$  glasses), while intensity of the second crystallization reaction almost does not change (see Figure 5). In addition, a third crystallization reaction occurs in these two alloys just prior melting and the melting temperature increases with an increase in Al content. The first melting reaction in the alloys with 10 and 15% Al starts rather slow; the reaction rate gradually increases to a maximum value and then abruptly decreases to almost zero. After that, a weak and shallow melting reaction is observed in a wide temperature range, probably due to gradual melting of a primary phase. Crystallization becomes even more complex in the  $\text{Ca}_{60}\text{Mg}_{18}\text{Al}_{15}\text{Zn}_3\text{Cu}_4$  glass with an increased amount of Ca and at least 5 crystallization exothermic peak are recognized on a DSC pattern of this alloy. The melting range in the quinary glasses is very wide, between  $112^\circ\text{C}$  for  $\text{Ca}_{60}\text{Mg}_{18}\text{Al}_{15}\text{Zn}_3\text{Cu}_4$  and  $221^\circ\text{C}$  for  $\text{Ca}_{55}\text{Mg}_{18}\text{Al}_{15}\text{Zn}_6\text{Cu}_6$ . This provides an opportunity to design even better glass forming alloys in this system by modifying the composition and reducing the temperature interval for melting (solidification).

## **Conclusions**

Several low density bulk metallic glasses were produced in Ca-Mg-Al, Ca-Mg-Al-Zn, Ca-Mg-Al-Cu and Ca-Mg-Al-Zn-Cu alloy systems. The maximum fully amorphous thickness of  $\tau_{\text{max}} = 9$  mm was achieved in a  $\text{Ca}_{55}\text{Mg}_{18}\text{Al}_5\text{Zn}_{11}\text{Cu}_{11}$  alloy. Two alloys,  $\text{Ca}_{60}\text{Mg}_{20}\text{Al}_{10}\text{Zn}_{10}$  and

$\text{Ca}_{55}\text{Mg}_{18}\text{Al}_5\text{Zn}_{11}\text{Cu}_{11}$  have  $\tau_{\max} = 5$  mm, eleven alloys have  $\tau_{\max}$  from 2 to 4 mm, and 5 alloys have  $\tau_{\max}$  of 1.0 to 1.5 mm. The compositions of these alloys provide efficiently packed cluster structure ~~(Dan to describe)~~. An addition of Al usually reduces the glass forming ability, but it improves the glass stability by increasing  $T_g$  and  $T_x$ . The glassy alloys developed in this work have a wide temperature interval for solidification, which indicates that their compositions are rather far from eutectic points. It is therefore expected that even better glass former can be found in these alloy systems by modifying the compositions in order to reduce the solidification temperature range.

### **Acknowledgements**

This work was conducted at the Air Force Research Laboratory, Materials and Manufacturing Directorate, under an on-site contract No. FA8650-04-D-5233.

### **References**

1. K. Amiya, A. Inoue, Mater. Trans. JIM 43 (2002) 81-84.
2. K. Amiya, A. Inoue, Mater. Trans. JIM 43 (2002) 2578-2581.
3. O.N. Senkov, J.M. Scott, MRS Proceedings, Vol. 806, Materials Research Society, Warrendale, PA, 2003, p.145-150.
4. O.N. Senkov, J.M. Scott, Mater. Letters, 58 (2004) 1375-1378.
5. O.N. Senkov, J.M. Scott, Scripta Materialia, 50 (2004) 449-452.
6. E.S. Park, D.H. Kim, J. Mater. Research, 19 (2004) 685-688.
7. F.Q. Guo, S.J. Poon, G.J. Shiflet, Appl. Phys Letters, 84 (2004) 37-39.
8. O.N. Senkov, J.M. Scott, J. Non-Cryst. Solids, 351 (2005) 3087-3094.
9. E.S. Park, W.T. Kim, D.H. Kim, Mater. Sci. Forum, 475-479 (2005) 3415-3418.
10. O.N. Senkov, D.B. Miracle, J.M. Scott, Intermetallics, 14 (2006) 1055-1060.
11. Z. Zhang, V. Keppens, O.N. Senkov, D.B. Miracle, Mater. Sci. Eng. A, (2006).
12. A Inoue, Acta Metarialia, 48 (2000) 279-306.
13. O.N. Senkov and D.B. Miracle, Mater. Res. Bull. 36 (2001) 2183-2198.
14. O.N. Senkov, D.B. Miracle, S. Rao, MRS Proceedings, Vol. 754, Materials Research Society, Warrendale, PA, 2003, p.145-150
15. O.N. Senkov and D.B. Miracle, US Patent No. 6,623,566; 23 September 2003.

16. D.B. Miracle and O.N. Senkov, *Mater. Sci. Eng. A347* (2003) 50-58.
17. D.B. Miracle, W.S. Sanders, O.N. Senkov, *Phil. Magazine*, 83 (2003) 2409-2428.
18. O.N. Senkov, D.B. Miracle, H.M. Mullens, *J. Appl. Physics*, 97 (2005) 103502.
19. D.B. Miracle, *Nature Materials*, 3 (2004) 697-702.
20. M.L. Morrison, R.A. Buchanan, O.N. Senkov, D.B. Miracle, P.K. Liaw, *Metall. Mater. Transactions A*, 37A (2006) 1239-1245.
21. B. R. Barnard, P. K. Liaw, R. A. Buchanan, O. N. Senkov, D. B. Miracle, Oxidation of Ca-based Bulk Amorphous Materials, The 5<sup>th</sup> International Conference on Bulk Metallic Glasses, Awaji, Japan, October 1-5, 2006.
22. J.M. Scott, J.E. Dahlman, O.N. Senkov, D.B. Miracle, Corrosion Resistance of Ca-Based Bulk Metallic Glasses, The 5<sup>th</sup> International Conference on Bulk Metallic Glasses, Awaji, Japan, October 1-5, 2006.
23. O.N. Senkov, J.M. Scott, and D.B. Miracle, *J. Alloys Compounds*, 2006.
24. S. Gorsse, G. Orveillon, O.N. Senkov, D.B. Miracle, *Physical Review B*, 73 (2006) 224202-1-9.

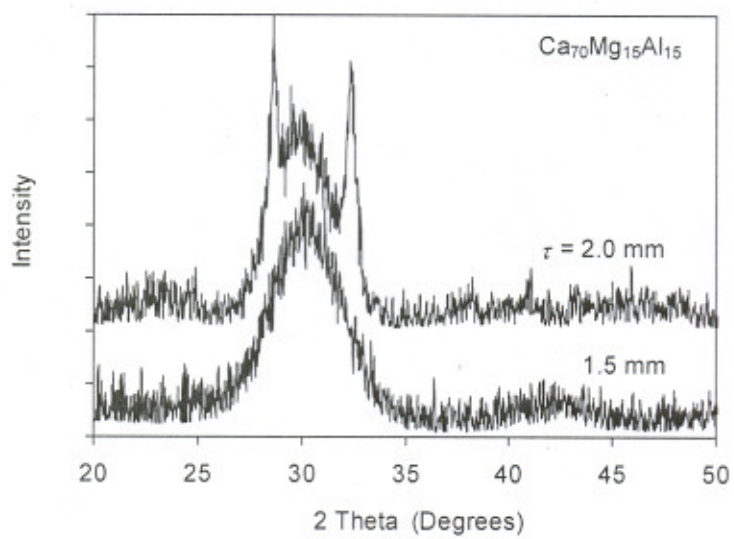


Table 1. Compositions (in at.%) of Ca-Mg-Al-based amorphous alloys and their glass transition,  $T_g$ , and crystallization,  $T_x$ , temperatures, the temperatures of start,  $T_m$ , and completion,  $T_l$ , of melting, and heats of crystallization,  $\Delta H_x$ , and melting,  $\Delta H_m$ , as well as the maximum thicknesses at which these alloys remain fully amorphous during copper mold casting.

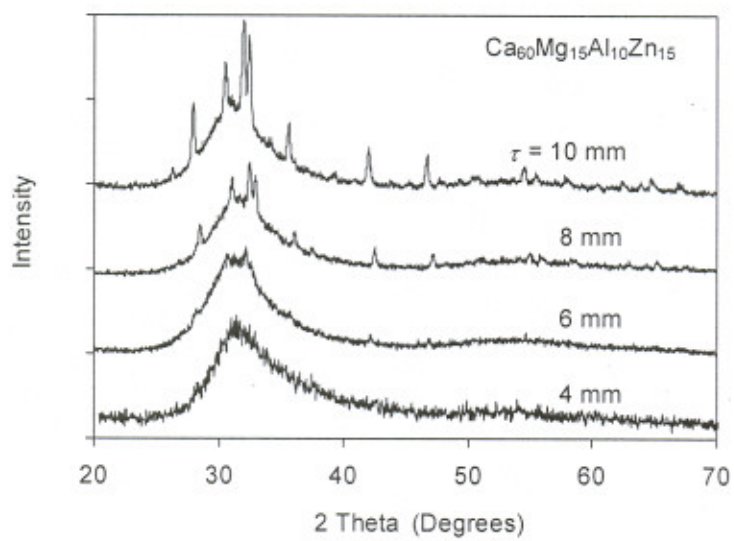
Composition (at.%)	$\rho$ (g/cc)	$\tau_{max}$ (mm)	$T_g$ (°C)	$T_x$ (°C)	$T_m$ (°C)	$T_l$ (°C)	$\Delta H_x$ (J/g)	$\Delta H_m$ (J/g)
Ca <sub>50</sub> Mg <sub>15</sub> Al <sub>35</sub>	1.79	<0.5	225	282	485	>600	96	>219
Ca <sub>55</sub> Mg <sub>15</sub> Al <sub>30</sub>	1.75	0.5	240	276	473	>600	104	>275
Ca <sub>60</sub> Mg <sub>15</sub> Al <sub>25</sub>	1.71	0.7	220	246	454	>600	153	>280
Ca <sub>62</sub> Mg <sub>9</sub> Al <sub>29</sub>	1.73	0.5	234	254	475	600	124	309
Ca <sub>65</sub> Mg <sub>15</sub> Al <sub>20</sub>	1.68	1.0	190	218	413	503	175	271
Ca <sub>70</sub> Mg <sub>15</sub> Al <sub>15</sub>	1.65	1.5	147	187	414	498	146	213
Ca <sub>70</sub> Mg <sub>26</sub> Al <sub>4</sub>	1.60	<0.5		225	358	540	-	207
Ca <sub>72.5</sub> Mg <sub>12.5</sub> Al <sub>15</sub>	1.64	0.5	144	181	367	508	177	290
Ca <sub>75</sub> Mg <sub>15</sub> Al <sub>10</sub>	1.62	0.5	130	152	367	471	113	214
Ca <sub>48</sub> Mg <sub>13</sub> Al <sub>19</sub> Zn <sub>20</sub>	2.26	0.5	163	214	375	540	70	114
Ca <sub>55</sub> Mg <sub>18</sub> Al <sub>20</sub> Zn <sub>7</sub>	1.88	1	174	218	352	549	76	189
Ca <sub>55</sub> Mg <sub>20</sub> Al <sub>10</sub> Zn <sub>15</sub>	2.03	3.5	130	196	358	500	76	179
Ca <sub>55</sub> Mg <sub>20</sub> Al <sub>15</sub> Zn <sub>10</sub>	1.93	2	148	204	334	533	91	262
Ca <sub>55</sub> Mg <sub>20</sub> Al <sub>19</sub> Zn <sub>6</sub>	1.85	1.5	175	211	358	472	92	223
Ca <sub>60</sub> Mg <sub>15</sub> Al <sub>10</sub> Zn <sub>15</sub> *	2.01	4	130	201	350	430	99	124
Ca <sub>60</sub> Mg <sub>18</sub> Al <sub>15</sub> Zn <sub>7</sub>	1.84	2.5	158	212	348	475	110	203
Ca <sub>60</sub> Mg <sub>20</sub> Al <sub>10</sub> Zn <sub>10</sub> ♦	1.89	5	130	176	334	473	95	181
Ca <sub>50</sub> Mg <sub>20</sub> Al <sub>10</sub> Cu <sub>20</sub>	2.22	1	138	168	384	458	96	227
Ca <sub>50</sub> Mg <sub>22.5</sub> Al <sub>5</sub> Cu <sub>22.5</sub>	2.27	3.5	143	183	354	489	100	188
Ca <sub>60</sub> Mg <sub>9</sub> Al <sub>11</sub> Cu <sub>20</sub>	2.17	2	128	177	383	484	117	185
Ca <sub>60</sub> Mg <sub>15</sub> Al <sub>10</sub> Cu <sub>15</sub>	2.03	2	124	157	384	537	103	165
Ca <sub>60</sub> Mg <sub>20</sub> Al <sub>10</sub> Cu <sub>10</sub>	1.90	2	135	169	390	544	96	210
Ca <sub>55</sub> Mg <sub>18</sub> Al <sub>5</sub> Zn <sub>11</sub> Cu <sub>11</sub>	2.22	9	119	175	331	513	114	192
Ca <sub>55</sub> Mg <sub>18</sub> Al <sub>10</sub> Zn <sub>11</sub> Cu <sub>6</sub>	2.09	3	128	171	341	562	101	228
Ca <sub>55</sub> Mg <sub>18</sub> Al <sub>15</sub> Zn <sub>6</sub> Cu <sub>6</sub>	1.99	2.5	136	177	360	581	95	293
Ca <sub>60</sub> Mg <sub>18</sub> Al <sub>10</sub> Zn <sub>6</sub> Cu <sub>6</sub>	1.94	5	134	176	357	530	128	211
Ca <sub>60</sub> Mg <sub>18</sub> Al <sub>15</sub> Zn <sub>3</sub> Cu <sub>4</sub>	1.84	2	144	195	370	503	123	193

\* The alloy is more than 80% amorphous at the thickness of up to 10mm.

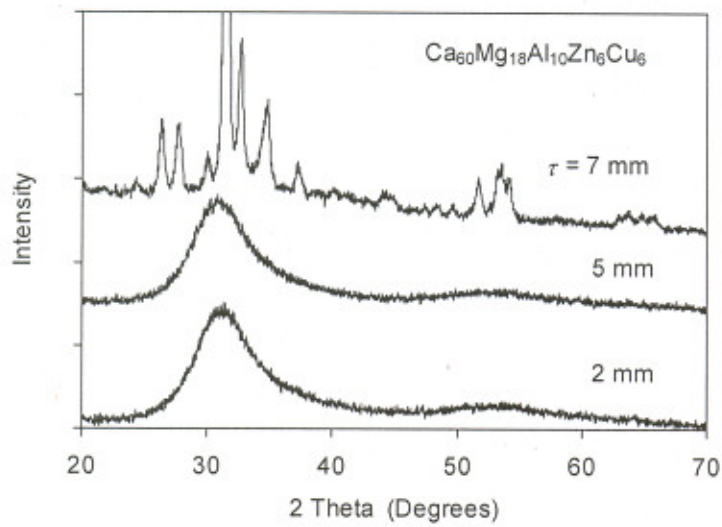
♦ The alloy is more than 80% amorphous at the thickness of up to 8 mm.



(a)



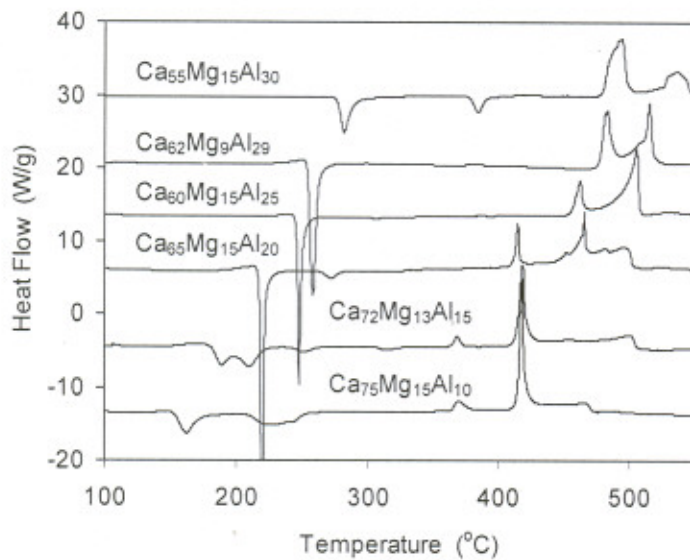
(b)



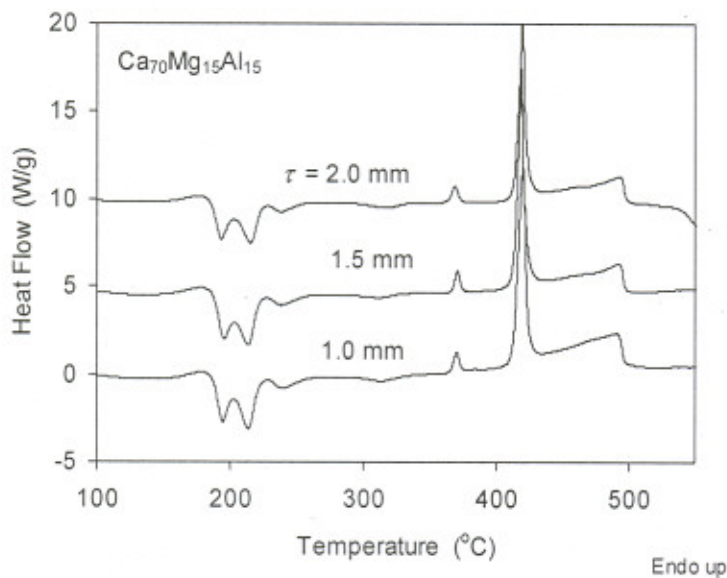
(c)

Figure 1. Typical X-ray diffraction patterns of amorphous and semiamorphous samples extracted from the regions of different thicknesses (shown in the figures) of the copper mold wedge cast alloys (a)  $\text{Ca}_{70}\text{Mg}_{15}\text{Al}_{15}$ , (b)  $\text{Ca}_{60}\text{Mg}_{15}\text{Al}_{10}\text{Zn}_{15}$  and (c)  $\text{Ca}_{60}\text{Mg}_{18}\text{Al}_{10}\text{Zn}_6\text{Cu}_6$ .





(a)



(b)

Figure 2. DSC patterns of amorphous samples extracted from (a) the regions of the maximum amorphous thicknesses of different Ca-Mg Al- alloys (their compositions are shown in the figure) and (b) the regions of different thicknesses of a  $\text{Ca}_{70}\text{Mg}_{15}\text{Al}_{15}$ . The wedge-like alloys were prepared by casting in a water-cooled copper mold. The DSC patterns were obtained during continuous heating at a heating rate of  $40^\circ\text{C}/\text{min}$  and endothermic reactions are directed up.

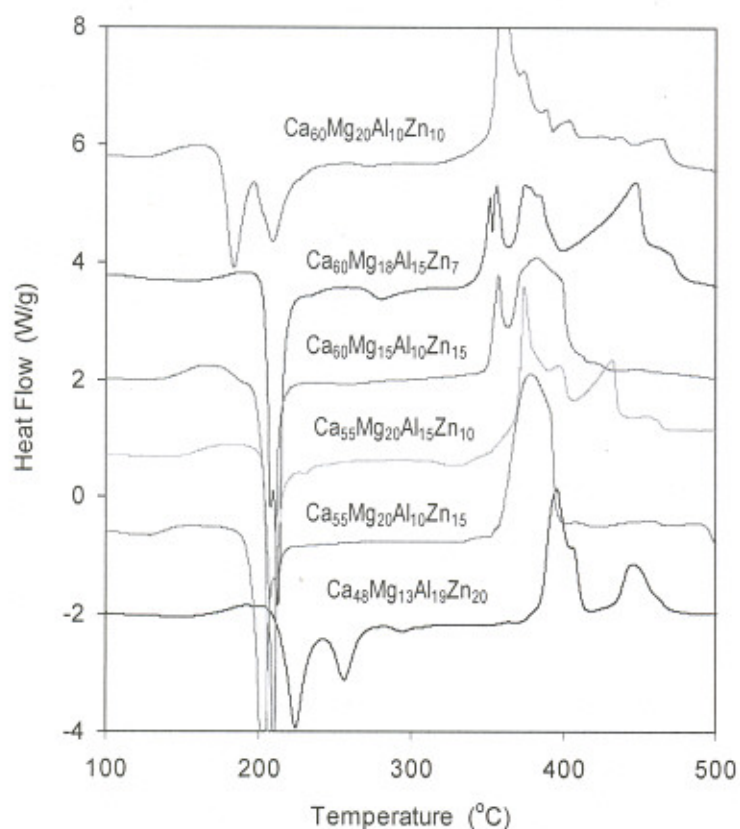


Figure 3. DSC patterns of amorphous samples extracted from the regions of maximum amorphous thicknesses of the copper mold wedge cast Ca-Mg Al-Zn alloys. The alloy compositions are shown in the figure and their glass transition, crystallization and melting temperatures, as well as maximum amorphous thicknesses, are given in Table 1. The DSC patterns were obtained during continuous heating at a heating rate of 40°C/min and endothermic reactions are directed up.

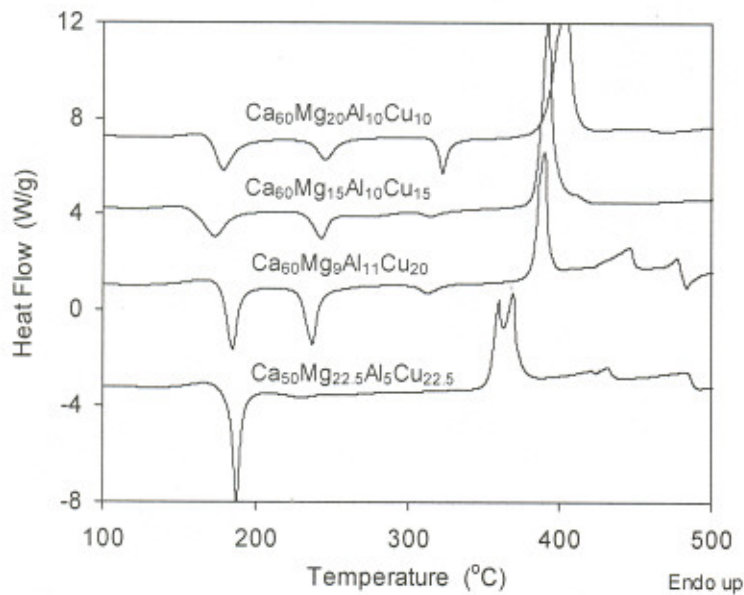


Figure 4. DSC patterns of amorphous samples extracted from the regions of maximum amorphous thicknesses of the copper mold wedge cast Ca-Mg Al-Cu alloys. The alloy compositions are shown in the figure and their glass transition, crystallization and melting temperatures, as well as maximum amorphous thicknesses, are given in Table 1. The DSC patterns were obtained during continuous heating at a heating rate of 40°C/min and endothermic reactions are directed up.



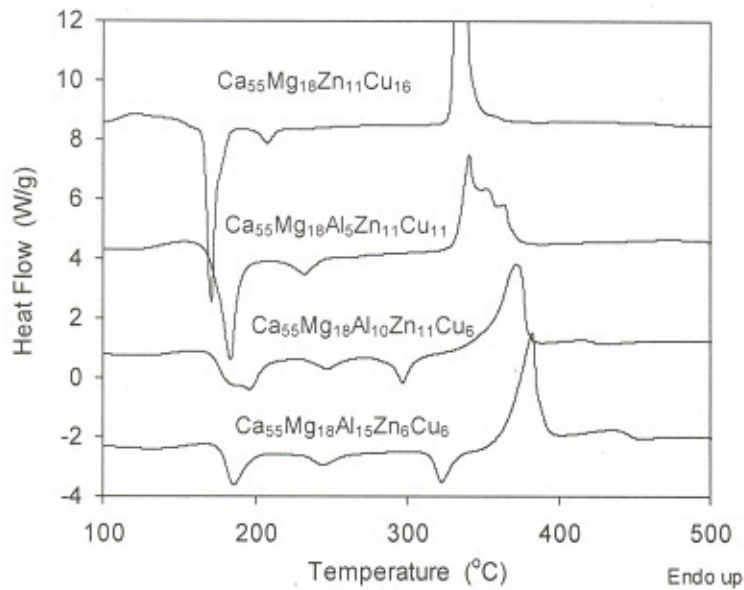


Figure 5. DSC patterns of amorphous samples extracted from the regions of maximum amorphous thicknesses,  $\tau_{\max}$ , of the copper mold wedge cast Ca-Mg Al-Zn-Cu alloys. The alloy compositions are shown in the figure and their glass transition, crystallization and melting temperatures are given in Table 1. A DSC pattern from a base-line  $\text{Ca}_{55}\text{Mg}_{18}\text{Zn}_{11}\text{Cu}_{16}$  glassy alloy with  $\tau_{\max} = 10$  mm is also shown. The DSC patterns were obtained during continuous heating at a heating rate of  $40^\circ\text{C}/\text{min}$  and endothermic reactions are directed up.